TASK II

Project II.2

MICROSCALE SIMULATION OF HIGH PRESSURE THERMAL AND CATALYTIC CONVERSION PROCESSES IN COAL AND WASTE POLYMERS WITH ON-LINE GC/MS

Henk L. C. Meuzelaar, Kui Liu, Wen Hu Du, Emma Jakab
Center for Micro Analysis and Reaction Chemistry
University of Utah

Microscale Hydropyrolysis Simulation by High Pressure TG/GC/MS
(Kui Liu, Wen Hu Du)

The high pressure TG/GC/MS system is shown in Figure IV.2.1. The quartz crucible holding the sample was modified as illustrated. The open hole in the bottom increases the sensitivity of the system by a factor 5-10, thus permitting the use of smaller samples. The thermal decomposition of Blind Canyon DECS-6 coal as well as of 1:1 mixtures of coal with polymer samples was studied under various conditions as listed in Table IV.2.I. The catalyst used was 1% Fe as iron chloride hexahydrate [$FeCl_3 \cdot 6H_2O$] promoted with 0.05% Mo in the form of ammonium tetrathiomolybdate [$(NH_4)_2MoS_4$], as prepared and provided by Dr. Anderson and his co-workers. The thermogravimetric profiles in Figure IV.2.2 illustrate the effects of hydrogen and of catalyst on the decomposition of the original coal samples. The effect of hydrogen is clearly visible as a significant increase in volatiles evolution above 500 C. Adding catalyst to the coal increases the total weight loss (Table IV.2.1) by about 3-4% and, as expected, the volatiles evolution occurs at lower temperatures.

The total ion intensity profile of coal obtained in helium (thermolysis) be seen in Figure IV.2.3a indicating that the maximum rate of decomposition occurs at 480 C. Enlarging one sampling period, the total ion curve shows the separation of several compounds within the 1.22 min interval (Figure IV.2.3b). Although the resolution is insufficient in the

low MW range due to the relatively high column temperature (90 C), the extracted single ion chromatograms can be used for further analysis. Figures IV.2.3c and d show the abundance of characteristic alkenyl type (m/z 55) and alkyl type (m/z 57) fragment ions revealing the increase in alkene/alkane ratio with decreasing carbon atom number. The intensity profile of a typical alkyl phenol fragment ion (m/z 107) indicates (Figure IV.2.3e) that not only different compounds with different MW values (e.g. cresol vs. xylenol), but also certain isomers (e.g. ethyl phenol vs. dimethyl phenol) can be separated on the short column.

Figure IV.2.4 shows the effect of hydrogen reactant gas and a liquefaction catalyst on the evolution profiles of four characteristic coal conversion products. The TG curve (Figure IV.2.2) exhibits two main decomposition regions in a hydrogen atmosphere (350-520 C and $\geq$520 C). The rate of volatile evolution up to 520 C is similar in hydrogen and helium suggesting that hydrogen does not promote the devolatilization significantly in this temperature range. This assumption is confirmed by the intensity profiles of the individual ions in Figure IV.2.4. Although there are some variations in the evolution curves the overall difference does not seem to be significant in the lower temperature range. However, the formation of alkyl aromatic products (m/z 92, toluene and m/z 142, methyl naphthalene) is greatly enhanced at high temperatures in a hydrogen atmosphere. The liquefaction catalyst applied in hydrogen atmosphere increases the yield of each product. Some increase is observed in the high temperature release of alkyl aromatics in comparison with the uncatalyzed coal experiment in hydrogen. Furthermore, the catalyst promotes the formation of alkanes (as judged by the m/z 43 propyl fragment ion) and phenol (m/z 94) as well as of methyl naphthalenes at lower temperatures.

To the best of our knowledge, this is the first time that the effects of hydrogen and catalyst on coal conversion processes have been successfully observed by on-line

chromatographic and spectroscopic analysis of characteristic conversion products. Although many more experiments, (e.g. involving different coals and catalysts as well as comparisons with off-line analysis results from bench scale hydropyrolysis processes) need to be performed in order to validate this technique, our preliminary data with regard to specificity and reproducibility suggest that HPTG/GC/MS offers an attractive approach to screening of catalysts and, perhaps, optimization of reaction parameters. In order to determine the usefulness of the method for simulating conversion of coal/waste polymer mixtures several different polymers (polyethylenes, polystyrene) and a sample of tire rubber were analyzed in neat form, as illustrated by the TG profiles in Figure IV.2.5.

Figure IV.2.6 shows the average mass spectra of the volatiles evolved from 350 to 600 C from coal and rubber as well as coal + rubber, with and without catalyst in a hydrogen atmosphere. The spectrum of the high volatile bituminous coal is dominated by alkenyl (m/z 41, 55, 69, 83, etc.), and alkyl (m/z 43, 57, 71, 85, etc.) type fragment ion series as well as aromatic hydrocarbons (m/z 78, benzene; m/z 91, toluene fragment ion) and phenols (m/z 94, phenol; m/z 107, cresol fragment ion). The rubber spectrum shows the formation of unsaturated hydrocarbon ions from the butadiene segments of rubber (e.g. m/z 67, methyl butadiene fragment ion) and aromatic hydrocarbons originating from the styrene moieties (e.g. m/z 91, toluene fragment ion; m/z 104, styrene). It should be noted that the oil additive of rubber may also release aromatic products. The spectra of the coal + rubber mixture (1:1 ratio) resemble the rubber spectrum at first sight because the rubber releases higher amounts of organic volatiles than the coal. The evaluation of average mass spectra is further complicated by the formation of several common products from coal and rubber (e.g. alkyl aromatics and alkenes). In spite of these difficulties it can be seen that the intensity of several ions is not additive and the presence of catalyst changes the product distribution.

More detailed information can be obtained about the effect of waste rubber and catalyst on coal hydropyrolysis by using time-resolved data. Figure IV.2.7 compares the evolution profiles of m/z 92 and m/z 94 from coal, rubber and the 1:1 mixture. The absolute intensities cannot be directly compared due to the different experimental conditions; therefore the intensities are scaled for equal height. The toluene evolution profile of the mixture (Figure IV.2.7a) appears to be the sum of the individual components. Other hydrocarbons exhibit similar behavior, however, it should be emphasized that this is not yet a quantitative comparison.

The spectra of both coal and rubber contain the m/z 94 ion, however, it represents two different compounds, phenol and heptatriene, respectively. Due to the chromatographic separation, the intensity profile of each product can be monitored separately in the mixture, as seen in Figure IV.2.7b. The heptatriene evolution occurs at about the same temperature from the rubber and the mixture. The rate of phenol formation from coal shows two maxima in hydrogen atmosphere (at about 450 C and 550 C). The presence of rubber significantly promotes the release of phenol in the lower temperature range (350-520 C).

Hydroliquefaction Microreactor with On-line GC/MS
(Emma Jakab)

An obvious shortcoming of the above described HPTG/GC/MS instrument is that only coal conversion reactions in gaseous environments can be studied, thus precluding true hydro liquefaction experiments, e.g. in the presence of donor solvent. Consequently, we are now undertaking the development of a high pressure tubing reactor (HPTR) with on-line GC/MS capabilities. A similar reactor has been successfully used in our laboratory to study thermal cracking reactions in hydrocarbon jet fuels[1]. A schematic diagram of the system is shown in Figure IV.2.8. The HPTR/GC/MS system can tolerate the supercritical (or subcritical) solvent

rich environments that are often encountered in coal liquefaction processes, and is easier to operate and maintain than the HPTR/GC/MS, albeit lacking the TG's capability to continuously measure remaining sample weight. The system can be operated at pressures up to 2000 psi, and temperatures up to 1000 C. The pressure of the reactor is maintained constant by a back pressure regulator. Catalytic coal liquefaction experiments with solvent such as tetralin and decalin are expected to start in the summer of 1993.

REFERENCES

1. Dworzanski, J.P.; Chapman, J.N.; Meuzelaar, H.L.C., *Prepr. Pap. Am Chem. Soc. Div. Fuel Chem.* 37 (1992), 424.

TABLE IV.2.1
Weight Loss Data for High Pressure TG

	Fe, No Catalyst	Reactant Gas	Weight Loss, %
Coal	No	He	36.6
Coal	No	H_2	54.6
Coal	Yes	H_2	57.9
Coal & Rubber	No	H_2	57.7
Coal & Rubber	Yes	H_2	61.8
Coal & Polystyrene	No	H_2	71.9
Coal & Plastic	No	H_2	74.1
Coal & Polyethylene	No	H_2	77.4
Rubber	No	He	66.6
Rubber	No	H_2	67.5

FIGURE CAPTIONS

Figure IV.2.1. Schematic of the High Pressure TG/GC/MS system.

Figure IV.2.2. TG curves of coal and rubber under various conditions at high pressure (900 psi).

Figure IV.2.3. Thermal decomposition of coal in helium atmosphere. Total ion intensity a) in the whole temperature range; b) in a single sampling interval. Ion intensity of c) m/z 55, alkene; d) m/z 57, alkane; e) m/z 107, cresol fragment.

Figure IV.2.4. Effect of hydrogen and catalyst on the evolution profile of coal conversion products. a) m/z 43, propyl fragment, b) m/z 94, phenol; c) m/z 92, toluene; d) m/z 142 methyl naphthalene.

Figure IV.2.5. TG curves of 1:1 mixtures of coal with various polymers at high pressure (900 psi).

Figure IV.2.6. Average mass spectra of hydropyrolysis products of coal, rubber and coal + rubber with and without catalyst from 350 C to 600 C. (m/z 14, 28, 32, 40 are background peaks.)

Figure IV.2.7. Evolution profile of a) m/z 92, (toluene); b) m/z 94, (phenol and heptatriene) from the hydropyrolysis of coal, rubber and a 1:1 coal/rubber.

Figure IV.2.8. Schematic of the HPTR/GC/MS system under development for microscale simulation of hydroliquefaction reactions.

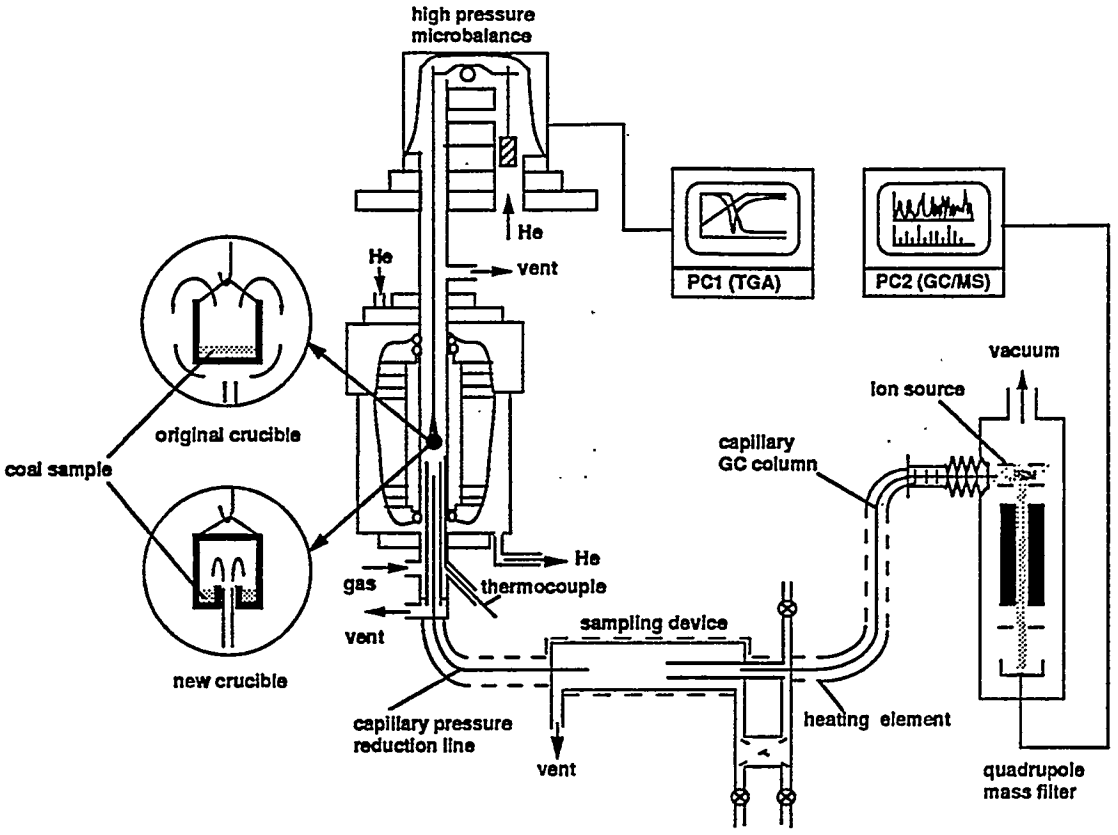

Figure IV.2.1. Schematic of the High Pressure TG/GC/MS system.

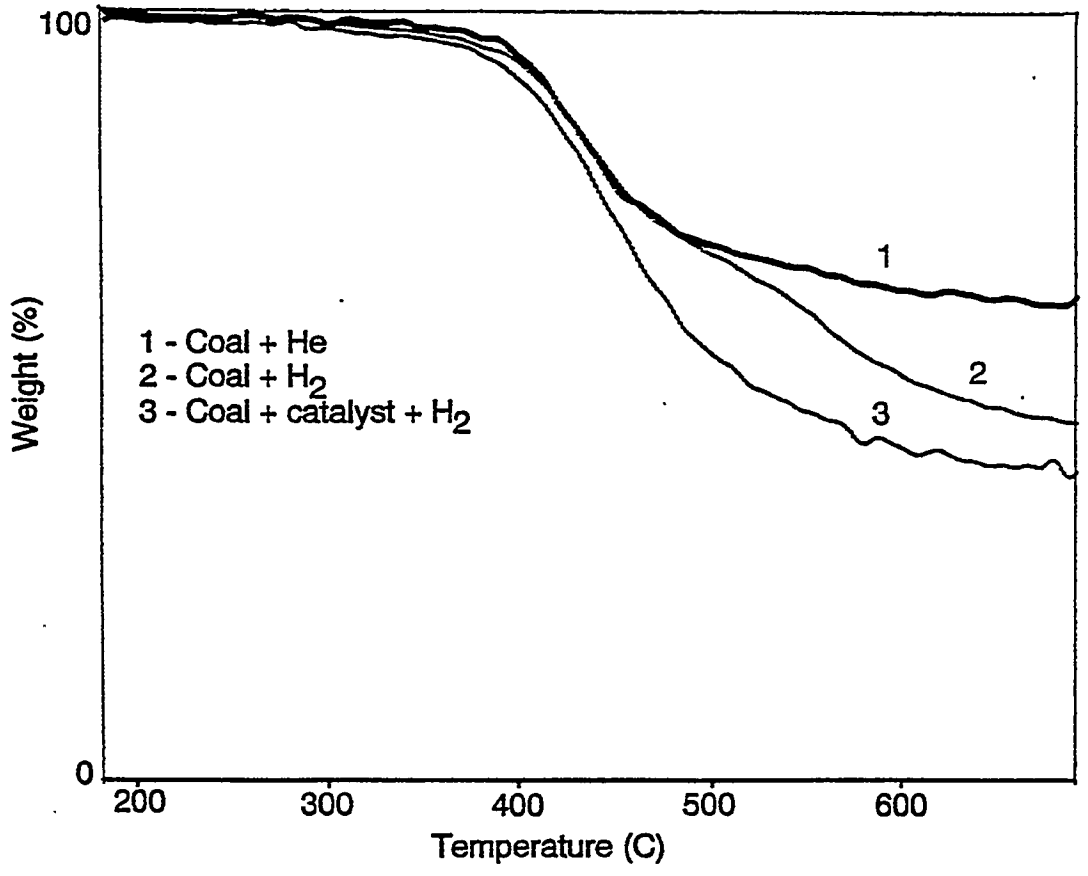

Figure IV.2.2. TG curves of coal and rubber under various conditions at high pressure (900 psi).

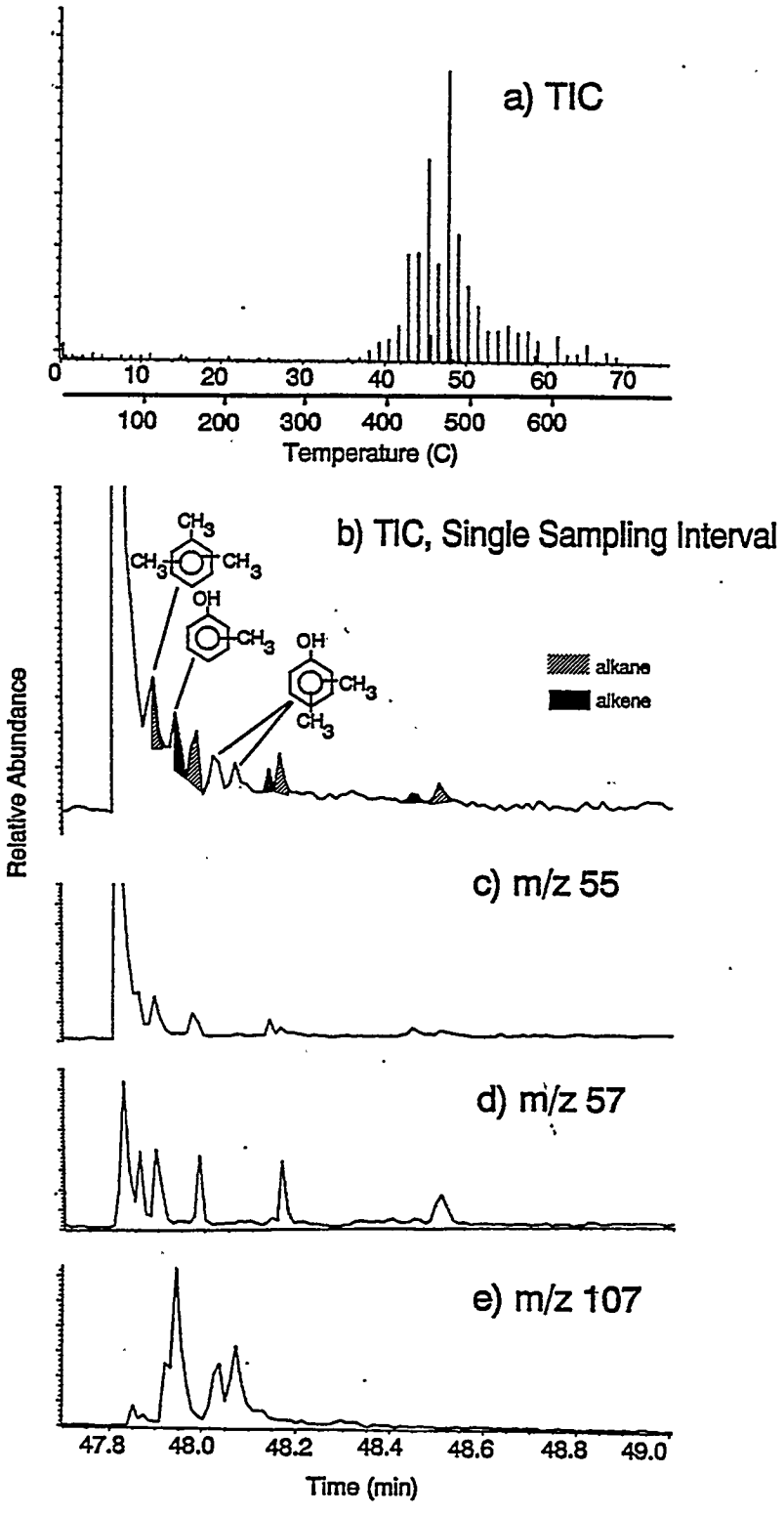

Figure IV.2.3. Thermal decomposition of coal in helium atmosphere. Total ion intensity a) in the whole temperature range; b) in a single sampling interval. Ion intensity of c) m/z 55, alkene; d) m/z 57, alkane; e) m/z 107, cresol fragment.

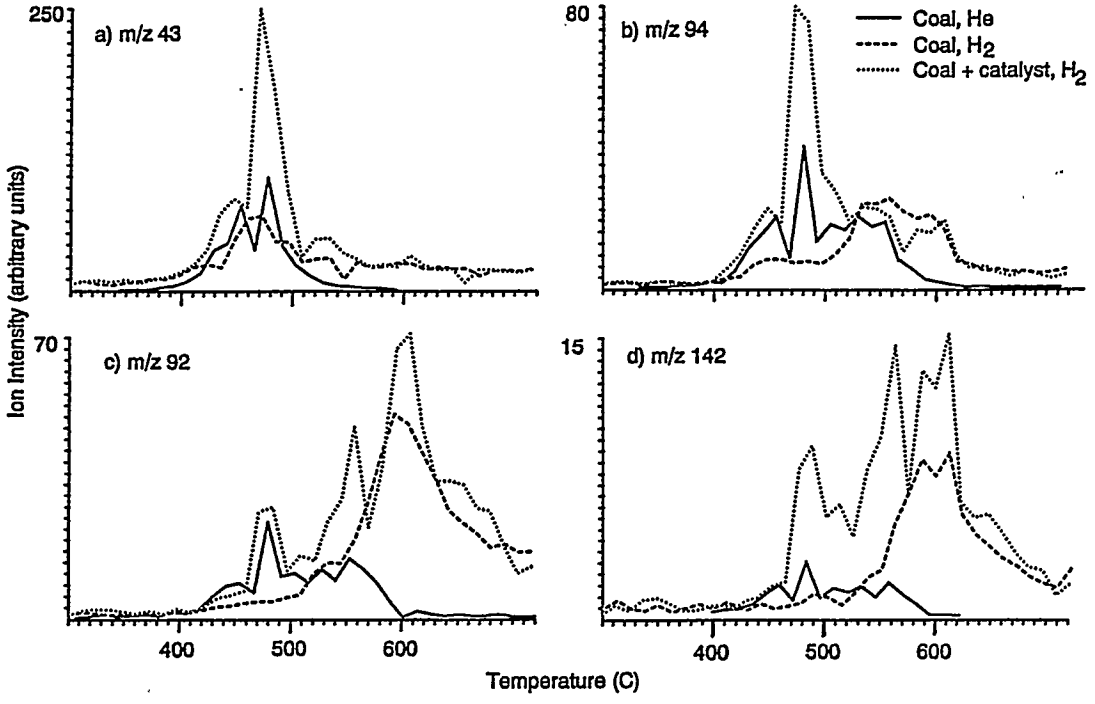

Figure IV.2.4. Effect of hydrogen and catalyst on the evolution profile of coal conversion products. a) m/z 43, propyl fragment, b) m/z 94, phenol; c) m/z 92, toluene; d) m/z 142 methyl naphthalene.

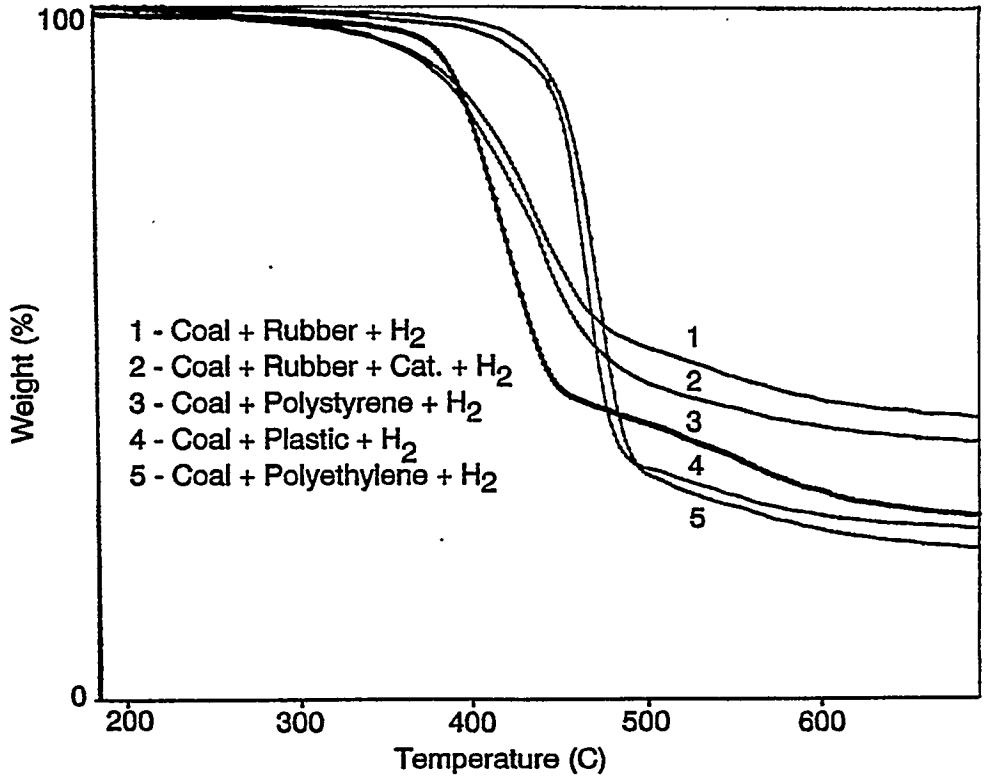

Figure IV.2.5. TG curves of 1:1 mixtures of coal with various polymers at high pressure (900 psi).

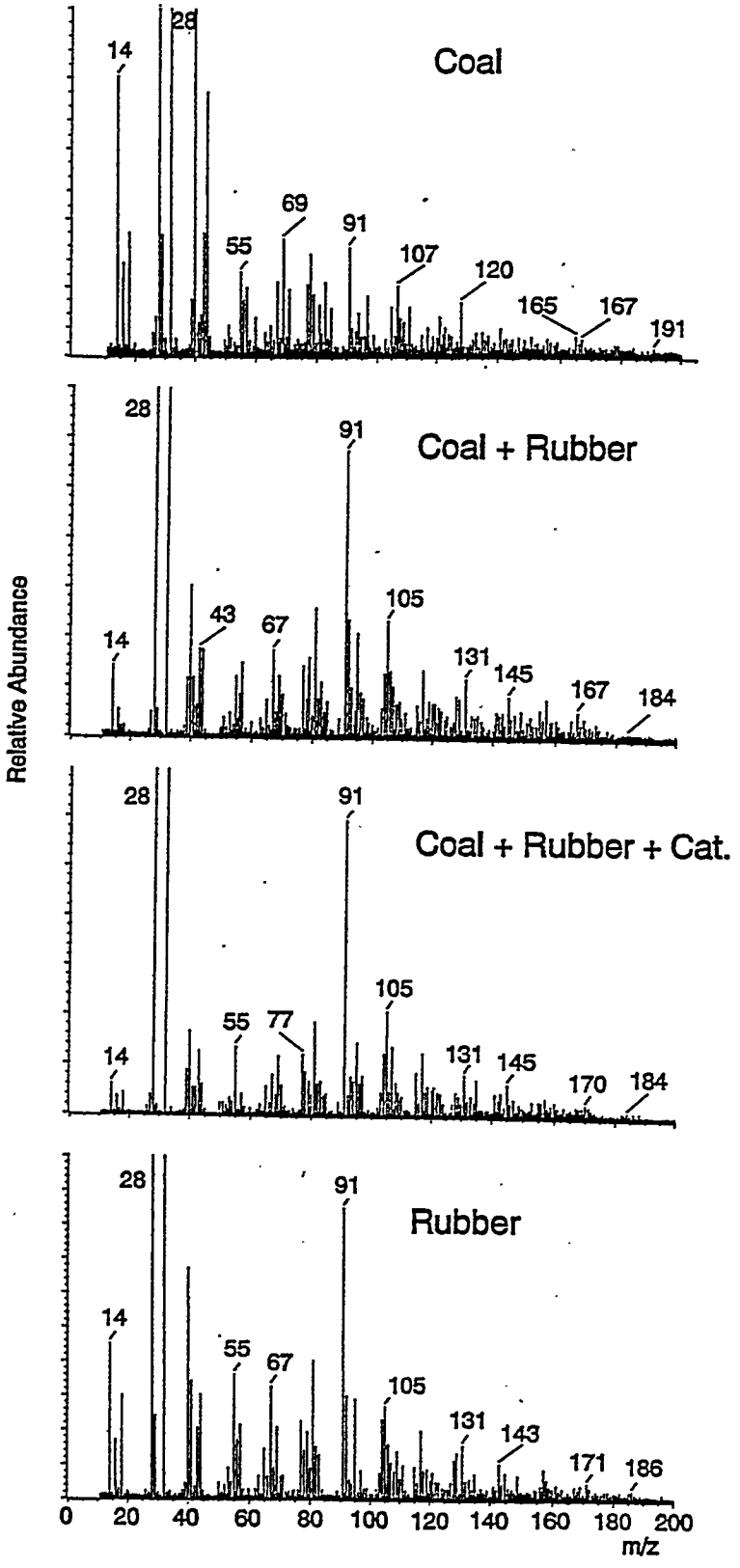

Figure IV.2.6. Average mass spectra of hydropyrolysis products of coal, rubber and coal + rubber with and without catalyst from 350 C to 600 C. (m/z 14, 28, 32, 40 are background peaks.)

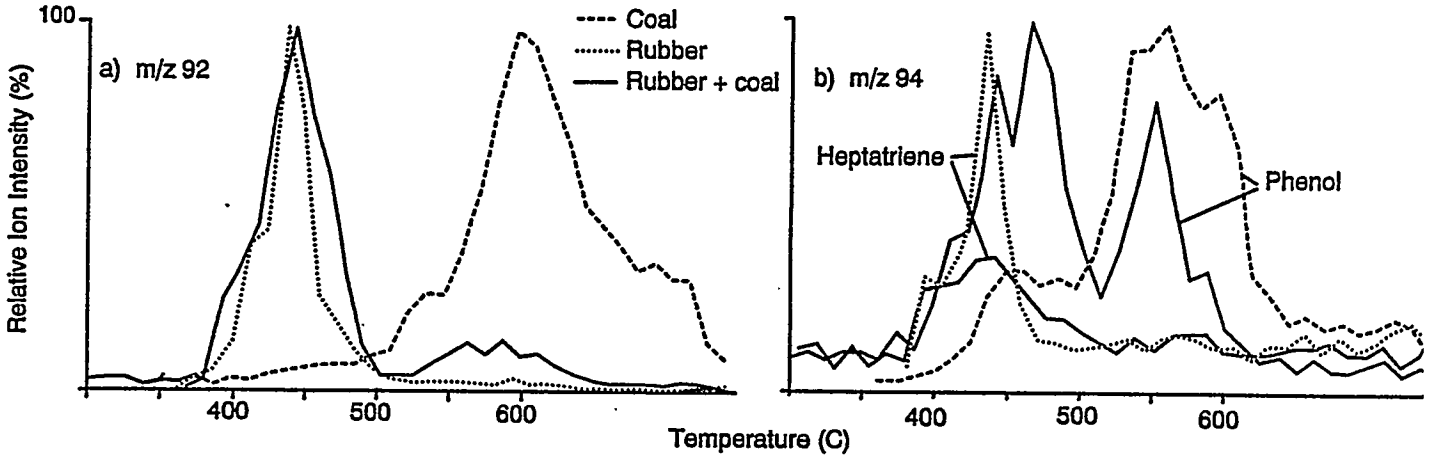

Figure IV.2.7. Evolution profile of a) m/z 92, (toluene); b) m/z 94, (phenol and heptatriene) from the hydropyrolysis of coal, rubber and a 1:1 coal/rubber.

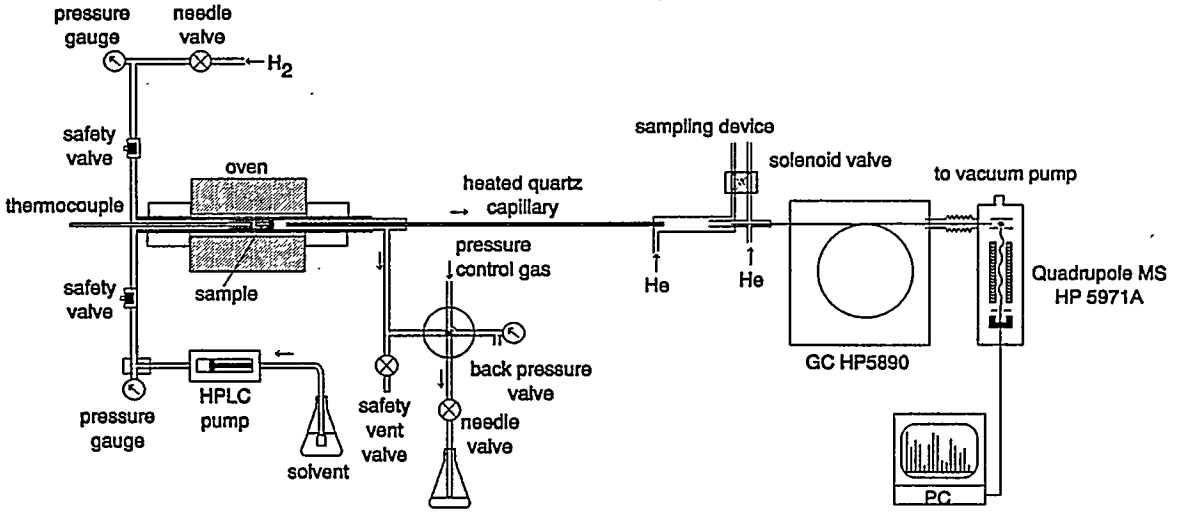

Figure IV.2.8. Schematic of the HPTR/GC/MS system under development for microscale simulation of hydroliquefaction reactions.

TASK II

Project II.3

CATALYTIC CRACKING, HYDROGENATION AND LIQUEFACTION OF COALS UNDER MILD CONDITIONS

Mohindar S. Seehra and Manjula M. Ibrahim
Department of Physics
West Virginia University

OBJECTIVES

For this period, the objectives of our project were as follows: (i) Determination of the particle size distribution of Fe-based coal liquefaction catalysts employing x-ray diffraction and squid magnetometry and (ii) Testing of these catalysts for liquefaction utilizing in-situ high temperature/high pressure electron spin resonance (ESR) spectroscopy. We also carried out some preliminary studies of coprocessing of coal with waste tires. Our research accomplishments in these tasks are presented below followed by a list of publications and conference presentations based on these studies.

SUMMARY OF RESULTS

(i) Catalyst characterization using x-ray diffraction and magnetometry:

The nine Fe-based catalysts used for these studies (provided by Dr. Wender's group) are listed in Table I. X-ray diffraction studies were carried out on a Rigaku diffractometer before and after drying the catalysts in air at 450°C for one hour. The positions of the Bragg peaks determine the chemical nature and widths of the peaks give the particle size. All the catalysts except Fe_7S_8 retained their chemical nature after drying, with only slight changes in particle size. On drying Fe_7S_8 showed conversion to α-Fe_2O_3. For a particular catalyst, the particle sizes determined from different Bragg lines vary somewhat, perhaps due to the irregular shapes of the particles. The average of particle sizes obtained from all the prominent peaks along with the standard deviations (representing the spread of values from different Bragg peaks) for the catalysts are presented in Table I. Magnetization measurements from 5 K to 300 K in zero-field-cooled and field-cooled cases are used to determine the

region of superparamagnetism, followed by magnetization measurements up to 55 kOe in the superparamagnetic state to determine the particle-size distribution [1]. The mean value of the particle sizes obtained from the magnetization data is also included in Table I.

Table I. List of the anion-modified iron oxide catalysts, their preparation routes [10,11] and their particle sizes determined from x-ray diffraction analysis. (NSP= not superparamagnetic up to 300K)

Catalyst	preparation route	Particle size (Å) x-ray	Magnetometry
Fe_2O_3/SO_4(1)	Homogeneous precipitation	110 ± 30	85 ± 5
Fe_2O_3/SO_4(2)	Rapid heterogen. precipitation	250 ± 35	NSP
$Mo/Fe_2O_3/SO_4$	Homogeneous precipitation	140 ± 45	100 ± 5
$Fe_2O_3/SnO_2/SO_4$	Heterogeneous precipitation	20 ± 5	95 ± 5
Fe_2O_3/MoO_4	Heterogeneous precipitation	140 ± 20	100 ± 5
Fe_2O_3/WO_4	Heterogeneous precipitation	290 ± 35	NSP
$FeOOH/SO_4$	Homogeneous precipitation	75 ± 25	95 ± 10
$Mo/FeOOH/SO_4$	Homogeneous precipitation	50 ± 20	100 ± 10
Fe_7S_8		400 ± 100	NSP

(ii) In-situ ESR spectroscopy to test the activities of the catalysts:

All the nine catalysts were tested for their hydrocracking abilities of Blind Canyon coal using in-situ high temperature ESR spectroscopy of coal free radicals. The details of the technique and procedures have been given in earlier publications [2-4]. The premise of this approach is based on the generally accepted view that the DCL involves the interaction of thermally/catalytically generated free radicals in coals with the available hydrogen [5] and that at least some of these radicals are detected by in-situ ESR spectroscopy [6]. Furthermore pyrolysis and hydrogenolysis is expected to increase the free radical density N whereas hydrogenation (which involves capping of the free radicals by captured hydrogen) is expected to lower N [5-8]. Thus efficiency and activity of a catalyst could be monitored by its effect on the free radical density N under different experimental conditions and the obtained results compared with the results of the more traditional liquefaction experiments. These results, described below, show that in-situ ESR spectroscopy of free radicals provides a promising technique for the testing of Fe-based catalysts.

The loading of the coal for all the experiments were in the ratio, Fe/coal = 1/99, Fe/S = 2, and in some experiments the solvent, 9,10 dihydrophenanthrene (DHP), was also added in the ratio DHP/coal = 2. To determine the changes in mass during heating, thermogravimetric (TG) measurements using Metler TA 3000 system, were done for coal alone and coal mixed with elemental S and the catalysts. Fig 1. shows the remaining weight obtained from TG for coal alone, coal loaded with the catalyst $Fe_2O_3/SO_4(1)$, and for coal loaded with the catalyst and sulfur. There is significant weight loss above 350°C, but the relative difference for the three cases is not significant. The TG data obtained for coal loaded with each of the catalysts is used in applying corrections for mass changes in the measurements of free radical densities (N is calculated per unit mass of the sample at the temperature of measurement.)

From ESR experiments the free radical densities are measured in-situ as a function of temperature in flowing hydrogen gas. The general features of the data are similar to those in bituminous coals [2-4] viz. a slight increase in N up to 100°C, followed by a decrease leading to a minimum near 300°C, and then a rapid increase in N due to thermal and catalytic cracking (stage 3). In some cases, at still higher temperatures, a fourth stage in which N again decreases with further increase in temperature also becomes evident [4].

We first consider the effect of a catalyst ($Fe_2O_3/SO_4(1)$) in the presence of elemental sulfur and DHP on the free radical density N of the Blind Canyon coal, at temperatures up to 550°C and in flowing H_2 gas, as shown in Fig. 2. As in earlier studies [2-4], the plotted $N = N_T(T/298)$ to take into account the Curie-law variation of the free radical density (N_T is the measured density at a temperature T and 298 K is the room temperature in degrees Kelvin). The results of Fig. 2 show that the addition of $Fe_2O_3/SO_4(1)$ and S results in an increase in N, the free radical density, especially above about 300°C. On the other hand, addition of DHP lowers N up to 280°C and above this temperature, there is no significant effect of DHP. A separate TG experiment with DHP showed that all DHP suddenly boils off at 280°C (inset of Fig 1). This explains the null effect of DHP above 280°C and the lower N (compared to coal) below 280°C is due to hydrogenation of the free radicals by DHP. Since DHP boils off in flowing H_2 experiments, the experiments with the remaining catalysts were carried out without DHP. This also eliminates the dominant hydrogenation characteristics of DHP and it provides a convenient technique to test relative effects of various catalysts as discussed below.

From the experiments of N vs T carried out with the catalysts of Table I, we have selected three catalysts, $Fe_2O_3/SO_4(1)$, Fe_2O_3/MoO_4, and $FeOOH/SO_4$ to present the typical results (Fig. 3) and the data on the Blind Canyon coal alone is also included for comparison purposes. This plot shows that in stage 3, above 300°C, the effect of the catalysts plus sulfur is to increase N at a given temperature, relative to the pure coal case. This additional increase in N can only be due to catalytic cracking in the presence of hydrogen and the magnitude of this effect is clearly different for different catalysts. This shows that this effect can be used to test the efficiency of different catalysts for hydrogenolysis or hydrocracking.

Most coal liquefaction experiments are carried out in the 350 to 450°C range and in our experiments reported here, significant changes in N are also observed in this region. To compare the catalytic cracking abilities of different catalysts, we compare the ratio $R = N_c/N_{coal}$ at 400°C, where N_c is the N value with a catalyst loading. If only thermal cracking is present, this ratio R will be unity. If $R < 1$, catalytic hydrogenation dominates and for $R > 1$, hydrogenolysis is occurring. This ratio R at 400°C for catalysts of Table I is plotted as a bar diagram in Fig. 4. Discussion of these results now follows.

The effects of the catalysts $Fe_2O_3/SnO_2/SO_4$ and Fe_2O_3/WO_4 on the free radical density N are similar to those of $Fe_2O_3/SO_4(1)$ (shown in Fig 3) in that catalytic cracking begins at the lower temperature of 280°C and the ratio R at 400°C is quite high (~2.4). Consequently, these may be considered as good hydrocracking catalysts. The effects of Fe_7S_8 and $Mo/Fe_2O_3/SO_4$ on the variation of free radical density with temperature are similar to Fe_2O_3/MoO_4 (shown in Fig 3). Here the ratio R at 400°C ~1.7 indicating that hydrocracking abilities of these catalysts are lower than those of $Fe_2O_3/SO_4(1)$, $Fe_2O_3/SnO_2/SO_4$ and Fe_2O_3/WO_4. On the other hand, the geothite based samples viz. $FeOOH/SO_4$ and $FeOOH/Mo/SO_4$ have essentially negligible catalytic activity and for these samples R is close to unity (R=1.3 for $FeOOH/SO_4$ and R=1 for $FeOOH/Mo/SO_4$) at all temperatures.

A major conclusion of the above results is that measurements of the free radical density N versus T and consequently the ratio R has provided a clear distinction between the effects of different catalysts. These conclusions can then be compared with the results of more traditional coal liquefaction experiments, whenever available. This comparison is discussed next using the results of Pradhan et al [9,10] who used these catalysts for the liquefaction of Blind Canyon coal at 400°C in 1000 psi of hydrogen and with tetralin as the donor solvent.

The work of Pradhan et al [9,10] showed that FeOOH-based catalysts in coal liquefaction experiments yield less oil as compared to experiments when Fe_2O_3-based catalysts are used. These findings are consistent with our results discussed above. Pradhan et al [9,10] attribute this difference to the fact that Fe_2O_3-based catalysts retain their small particle size better under liquefaction conditions while FeOOH agglomerates under these conditions. They also found that for the yield of oils, molybdated and tungstated hematite-based catalysts are better than sulfated iron oxides. Our ESR based results show Fe_2O_3/SO_4(1), Fe_2O_3/WO_4, and $Fe_2O_3/SnO_2/SO_4$ have the high R ratio of about 2.4 for hydrocracking, followed by R ~1.7 for Fe_2O_3/MoO_4, $Mo/Fe_2O_3/SO_4$ and Fe_7S_8. Although there is a general consistency among the two sets of experiments, we caution that hydrogenation effects of the catalysts, if present, would tend to lower the free radical density and hence the ratio R. Mo and W can form sulfides under liquefaction conditions which are strong hydrogenation catalysts, besides the hydrocracking abilities of the starting catalysts. This may be the reason for some of the minor discrepancies between the two sets of experiments. In our future work, we plan to test these catalysts with a hydrogen donor such as DHP under 600 psi pressure of hydrogen. With such experiments, we hope to separate the hydrocracking and hydrogenation effects.

The results presented here have demonstrated that the hydrocracking abilities of the different Fe-based catalysts for coal liquefaction can be quantified by the free radical density ratio R and that the conclusions drawn from the ratio R are in good agreement with those obtained from direct liquefaction experiments (e.g., both experiments show that geothite-based catalysts are less effective in coal liquefaction than oxide-based catalysts). In-situ x-ray diffraction experiments are needed to determine any chemical changes that the catalysts might undergo under liquefaction condition and ESR experiments under high pressure of hydrogen are needed to investigate the hydrogenation process. Both sets of these experiments are planned for the near future.

(iii) Investigation of the coprocessing of coal with waste tires by ESR spectroscopy and thermogravimetry:

We have investigated the coprocessing of coal with waste tire rubber employing thermogravimetry and in-situ ESR spectroscopy of free radicals. The tire polymer used in these experiments was chipped from a used tire (Goodyear Vector) and it was mixed with the coal in

1:1 ratio with mortar and pestle. Samples were cut from the center and rim portions of the tire and in separate TG and ESR experiments we did not find significant differences in the results between them. For the ESR experiments, samples were either vacuum sealed in the ESR tube at room temperature followed by measurements at elevated temperatures or measurements were done in flowing H_2 gas [2,3]. We also measured the weight loss in thermogravimetry in flowing H_2 gas using Mettler TA3000 system.

Fig. 5 shows the remaining weight (%) as a function of temperature for the Blind Canyon coal, the tire and the tire coal mixture in a flowing H_2 experiment. Most of the weight loss due to release of volatiles occurs between 300 and 500°C and it is clearly evident that the coal-tire mixture has the highest weight loss. If we use the weight loss due to volatiles as the percentage conversion, then at 500°C, the percentage conversions for coal, tire and coal-tire respectively are 32%, 48% and 66%. The presence of tire polymers has clearly enhanced the percentage conversion of coal.

In ESR spectroscopy, only a single line is observed from the coal sample and no ESR signal was observed from the tire as determined in a separate experiment up to 500°C. In Fig. 6, we show the temperature variation of the free radical density N for the coal and the coal-tire mixture in flowing H_2 gas. It is clearly evident that the tire has considerable effect on the coal free radicals. The following points are noteworthy.

At the lower temperatures of around 100°C, there is a slight increase in N due to the effect of tire. Above 400°C, the N values in the presence of tire polymer are suppressed by a factor of two to three. This rapid decrease in the free radical density at the higher temperatures (Fig. 6) is most likely due to hydrogenation facilitated by the transfer of hydrogen from tire polymers to coal fragments [8]. The liquefaction experiments of Farcasiu and Smith [11] carried out 425°C and those of Liu et al [12] at 400°C with waste tires also showed higher conversion of coal coprocessed with tires. Thus our results show that waste tires coprocessed with coal lower the free radical densities above 400°C, and increase the evolution of volatiles and that the tires act as excellent hydrogen donors.

Similar experiments in coprocessing coal with polyethylene and polystyrene indicated rapid hydrocracking of coal. These findings are positive indicators for improved liquefaction of coals in the presence of tires and polymers. These results on coprocessing coal with waste tires

and polyethylene and polystyrene have been communicated for publication in the forthcoming ACS preprints.

References:

1. Ibrahim M. M., Zhao J., and Seehra M. S., J. Mater. Res., 1992, 7, 1856-1860

2. Ibrahim, M. M. and Seehra, M. S., Am. Chem. Soc. Div. Fuel Chem. Preprints, 1992, 37, 1131-1140; ibid 1993, 38, 180-184.

3. Ibrahim, M. M. and Seehra, M. S., Energy & Fuels, 1991, 5, 74-78.

4. Seehra, M. S. and Ghosh, B., J. Anal. Appl. Pyrolysis, 1988, 13, 209-220.

5. Neavel, R. C., Fuel, 1976, 55, 237-242.

6. Petrakis, L. and Grandy, D. W. "Free Radicals in Coals and Synthetic Fuels", 1983 (Elsevier Science Publication Co., N.Y.).

7. Fowler, T. G., Bartle, K. D. and Kandiyoti, R., Fuel, 1987, 66, 1407-1412.

8. Shin, S.-C., Baldwin, R. M. and Miller, R. L., Energy & Fuels, 1989, 3, 71-76.

9. Pradhan, V. R., Hu, J., Tierney, J. W. and Wender, I., Am. Chem. Soc. Div. Fuel Chem. Preprints, 1993, 38, 8-13.

10. Pradhan, V. R., Hu, J., Tierney, J. W., and Wender, I., Energy & Fuels (in press).

11. Farcasiu, M.; Smith, C. ACS Fuel Div. Preprints 1992, 37, 472-479.

12. Liu, Z.; Zondlo, J. W.; Dadyburjor, D. B. (private communication).

Publications and Presentations:

M. M. Ibrahim, and M. S. Seehra; "Catalytic hydrogenation of Blind canyon coal studied by high temperature/ high pressure ESR Spectroscopy" Presented at the 66th Colloid and Surface Science Symposium, June 1992, Morgantown, West Virginia.

M. M. Ibrahim, and M. S. Seehra; "An apparatus for in-situ high temperature /high pressure ESR spectroscopy and its applications in coal conversion studies" ACS Division of Fuel Chem. Preprints, 1992, 37, p:1131-1140.

M. M. Ibrahim, J. Zhao, and M. S. Seehra; "Determination of particle size distribution in an Fe2O3-based catalyst using magnetometry and x-ray diffraction" J. Mater. Res., 1992, 7, p:1856-1860.

M. M. Ibrahim, and M. S. Seehra; "Hydrogenation of blind canyon coal monitored by high temperature/ high pressure ESR spectroscopy" Presented in the 6th Annual Technical Meeting, July 1992, Wheeling, West Virginia.

M. M. Ibrahim, and M. S. Seehra; "Free radical investigations of direct coal liquefaction with Fe-based catalysts using electron spin resonance spectroscopy", ACS Division of Fuel Chem. Preprints, (1993) 38, p:180-183.

G. P. Huffman, B. Ganguly, J. Zhao, K. Rao, N. Shah, Z. Feng, F. E. Huggins, M. M. Taghiei, F. Lu, I. Wender, V. R. Pradhan, J. W. Tierney, M. S. Seehra, M. M. Ibrahim, J. Shabtai and E. M. Eyring; "Structure and Dispersion of Iron-Based Catalysts for Direct Coal Liquefaction" , Energy & Fuels, 7, 285-296 (1993).

M. M. Ibrahim, and M. S. Seehra; "Testing Fe-based catalysts for direct coal liquefaction using in-situ electron spin resonance spectroscopy" (submitted to Energy & Fuels)

M. M. Ibrahim, and M. S. Seehra; "Thermogravimetric and free radical evidence for improved liquefaction of coal with waste tires" submitted to ACS meeting at Chicago to be held in August, 1993.

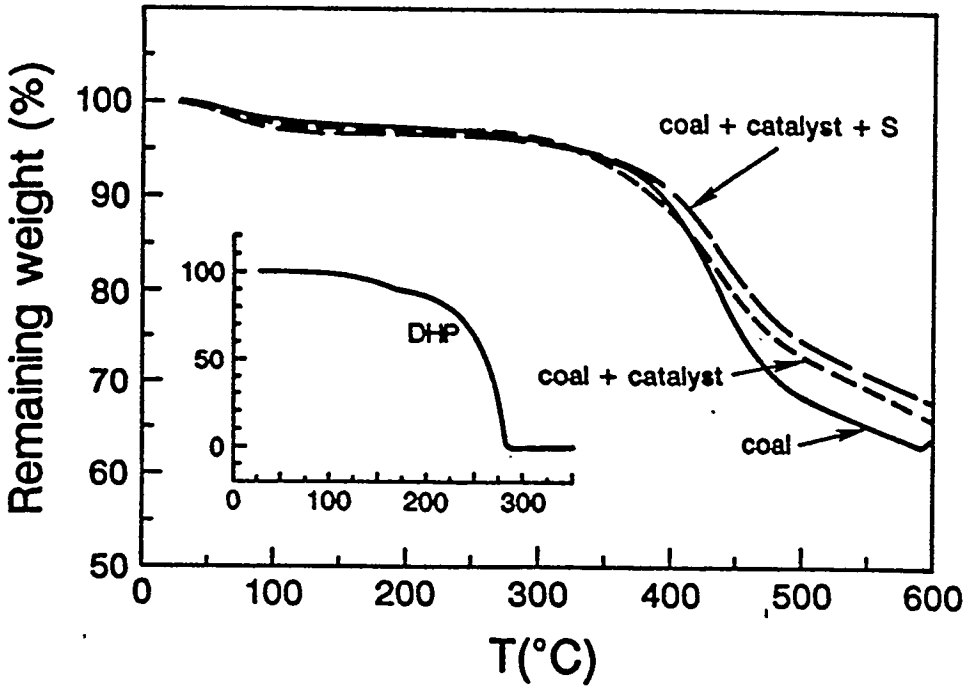

Fig. 1. Remaining weight(%) plotted as a function of temperature for coal, coal loaded with $Fe_2O_3/SO_4(1)$, and coal loaded with $Fe_2O_3/SO_4(1)$ and S. (The loadings were in the ratios, Fe/coal≃ 1%, Fe/S =1/2 and coal/DHP =1/2.) The inset shows rapid boiling of DHP by 280°C in hydrogen flow.

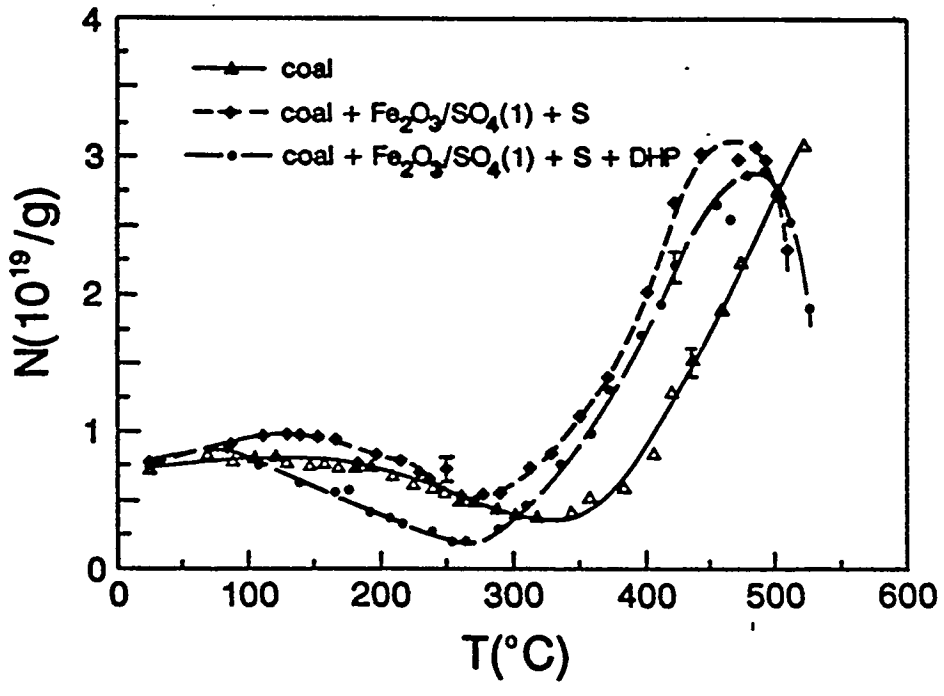

Fig. 2. Variation of free radical density, N for unloaded blind canyon coal, coal loaded with $Fe_2O_3/SO_4(1)$ and S, and coal loaded with $Fe_2O_3/SO_4(1)$, S and DHP.

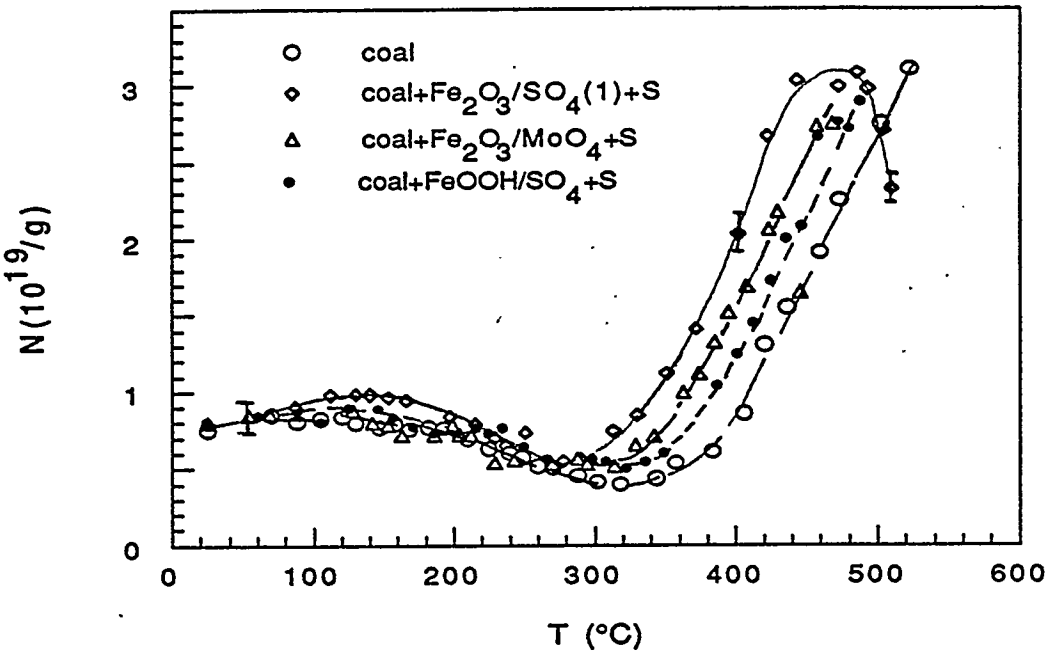

Fig. 3. Variation of N versus temperature for coal and coal loaded with $Fe_2O_3/S04$ (1), Fe_2O_3/MoO_4, and $FeOOH/SO_4$.

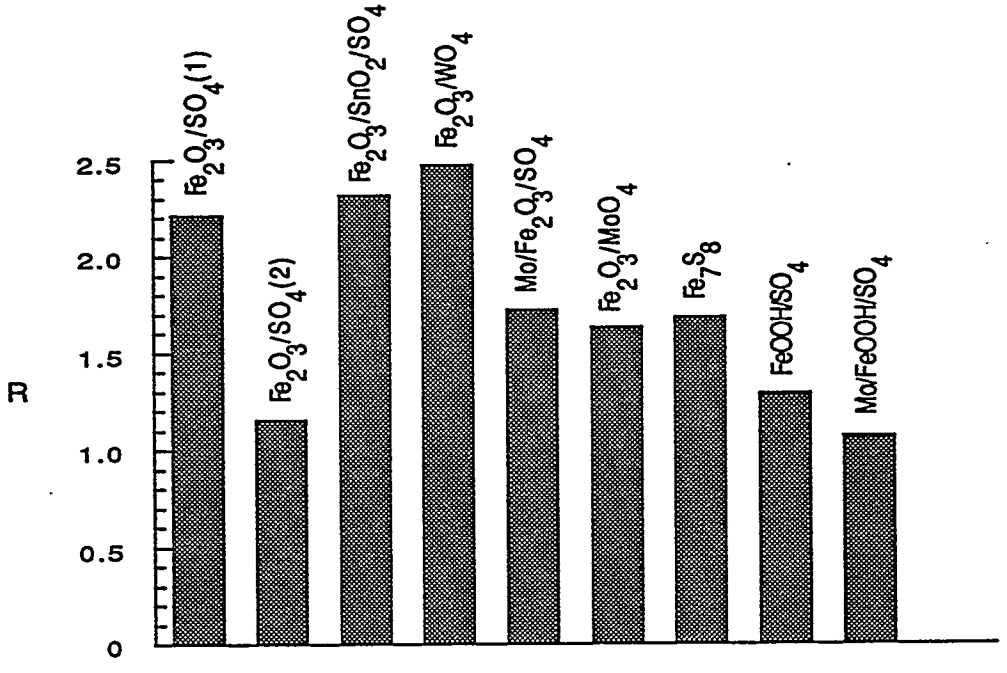

Fig. 4. The experimental ratio $R = N_C/N_{coal}$ at 400°C for different catalysts (N_C is the free radical density of a catalyst loaded coal).

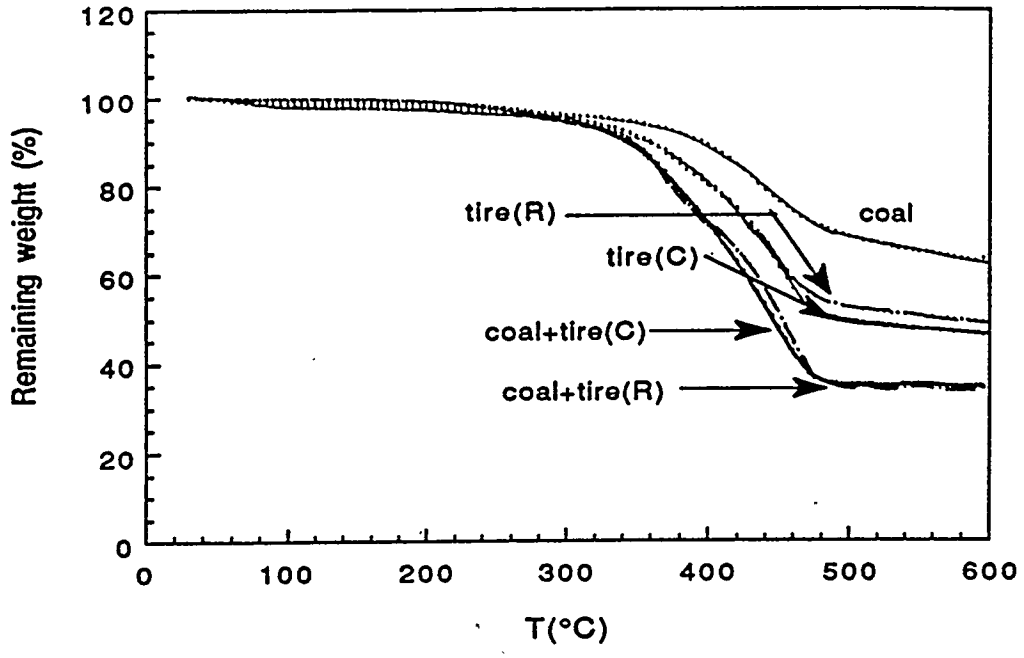

Fig 5. Remaining weight as a function of temperature for coal and coal tire mixtures (1:1 by weight). Tire(C) and tire(R) are cut from the central and rim portions of the tire. All measurements were done in flowing hydrogen.

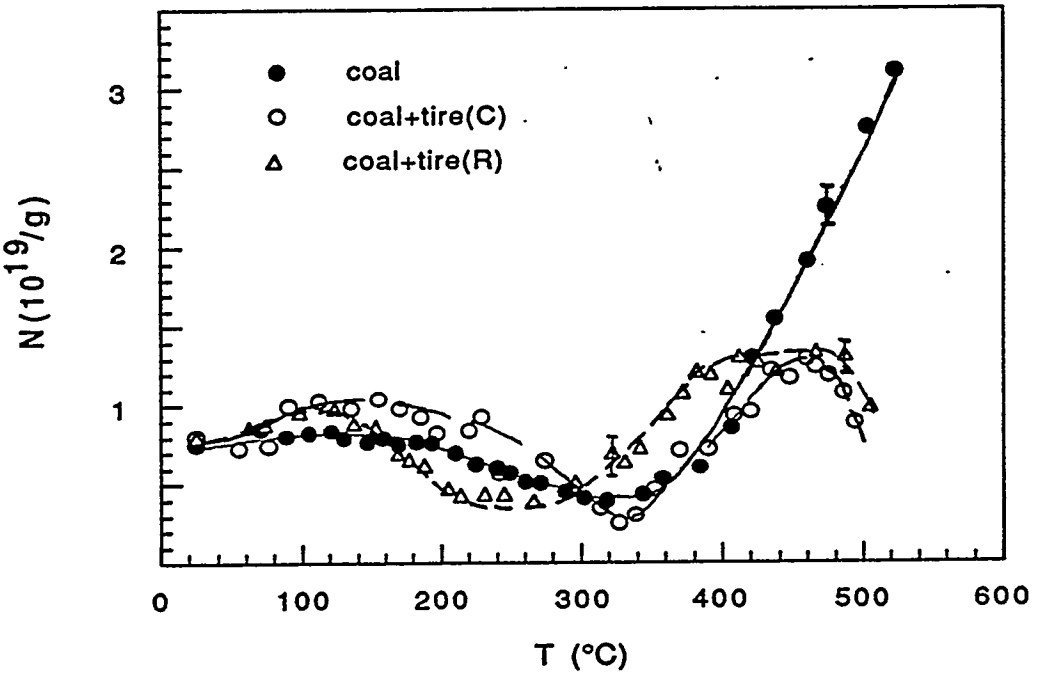

Fig. 6. Variation of free radical densities with temperature for coal and coal-tire mixtures (1:1 by weight). Measurements were done under hydrogen flow. Free radical densities are corrected for changes in mass.